Available online at www.sciencedirect.com
SCIENCE DIRECT®
ELSEVIER
Earth and Planetary Science Letters 219 (2004) 285–296
EPSL
www.elsevier.com/locate/epsl

$MgSiO_3$ phase boundaries measured in the laser-heated diamond cell

Liudmila Chudinovskikh, Reinhard Boehler *

Max-Planck-Institut für Chemie, Postfach 3060, 55020 Mainz, Germany

Received 24 July 2003; received in revised form 27 October 2003; accepted 1 December 2003

Abstract

New data on phase equilibria in the $MgSiO_3$ system relevant to the stability of Mg–Si-perovskite (perovskite) are obtained in the laser-heated diamond cell using improved techniques for accurate pressure measurement and novel heating techniques eliminating temperature gradients. The data of the $MgSiO_3$-ilmenite (akimotoite)–perovskite phase boundary, measured in the range of 19–25.5 GPa and 1800–2350 K, are consistent with the pressure and temperature conditions generally assumed at 660 km depth and agree within the experimental uncertainties with earlier multi-anvil quench experiments. The triple point wadsleyite+stishovite–akimotoite–perovskite is at 21 GPa and 2300 K. The slope of the akimotoite–perovskite boundary is not well constrained by reversal experiments alone due to large hysteresis, but results using glass starting materials yield a value of -0.004 ± 0.002 GPa/K. The slopes of the phase transitions to Mg–Si-perovskite in both olivine and pyroxene systems are less negative than those required to cause layering in mantle convection. At the pressure of the 660 km seismic discontinuity (23.8 GPa) the phase boundary between akimotoite and perovskite yields a slightly lower temperature than that of the ringwoodite to perovskite+periclase transition in the Mg_2SiO_4 system (1900 ± 100 K). Garnet (majorite) is not observed above 21 GPa.

Keywords: $MgSiO_3$; akimotoite; perovskite; phase boundaries; diamond cell; high pressure; laser heating

1. Introduction

It has long been recognized that the 660 km seismic discontinuity is linked to the transitions of open-structured silicate polymorphs to the dense perovskite structure [4,5] in both $MgSiO_3$ and Mg_2SiO_4 systems. The magnitude of this jump in seismic velocity may be due to a general change of the silicon–oxygen coordination from 4 to 6 at this pressure (23.8 GPa). Therefore, the pressure and temperature conditions of the phase boundary of Mg–Si-perovskite are crucial for estimating mineralogy and temperature in the Earth's mantle at 660 km depth [5,6]. Moreover, the Clapeyron slope of this phase boundary is of importance for geodynamical considerations because it determines the latent heat of the transition [7–10].

The phase boundary of Mg–Si-perovskite in both $MgSiO_3$ and Mg_2SiO_4 systems, extensively

* Corresponding author. Tel.: +49-6131-305-252; Fax: +49-6131-305-330.
E-mail addresses: chud@mpch-mainz.mpg.de (L. Chudinovskikh), boe@mpch-mainz.mpg.de (R. Boehler).

0012-821X/04/$ – see front matter © 2004 Elsevier B.V. All rights reserved.
doi:10.1016/S0012-821X(04)00005-6

measured in the laboratory using diamond-anvil and multi-anvil apparatuses, shows considerable variations in pressure, temperature, and slope [1–3,5,6,11–23]. The discrepancies may be mainly due to different methods of measuring pressure and temperature but phase kinetics may also play an important role. In multi-anvil in situ X-ray experiments the estimated pressures depend strongly on the choice of pressure standard and P–V–T equation of state used for pressure calibration. For $MgSiO_3$ the akimotoite to Mg–Si-perovskite transition pressures obtained from the latest in situ multi-anvil X-ray measurements [17,19–21] differ by as much as 2.5 GPa, depending on which equation of state of gold [24,25] or NaCl [26] is used. The reported discrepancies may not be solely caused by differences in the pressure calibration but also be due to the unknown pressure effect on the emf of W–Re thermocouples used in these studies [22,23,27]. Similar discrepancies for the Mg–Si-perovskite phase boundary between multi-anvil quench and in situ X-ray experiments have been observed for the olivine system [5,18,22,23] and for Al-bearing systems such as pyrope garnet ($Mg_3Al_2Si_3O_{12}$) [28,29] and natural pyrolite composition [22,27,30–32]. The uncertainties in pressure and temperature in both multi-anvil and diamond-anvil studies are discussed in numerous papers [2,3,17,18,21,22,27,29,33,34].

It has been shown recently that both pressures and temperatures can be measured accurately in the laser-heated diamond cell [33], and new techniques for measuring phase transitions of minerals using micro-furnaces in a hydrostatic, inert pressure medium have recently been developed [2]. This heating method essentially eliminates temperature gradient within the sample. Our recently reported measurements of the ringwoodite to Mg–Si-perovskite plus periclase transition in the Mg_2SiO_4 system [2] show excellent agreement with in situ synchrotron X-ray measurements in the laser-heated diamond cell [3].

2. Experimental methods and results

In the present study we report new data on the phase diagram of $MgSiO_3$ in the range of 18.5–25.5 GPa and 1800–2600 K measured for the first time in the diamond cell. $MgSiO_3$-glass samples with dimensions 10–15 μm were placed into metallic (rhenium or iridium) micro-furnaces embedded in an argon pressure medium and heated with two yttrium–lithium–fluoride (YLF) lasers (25 W Coherent and 50 W Quantronix, cw, TEM00) (Fig. 1A–D). Pressures listed in Table 1 were measured after heating from several ruby chips distributed in the argon pressure medium. These pressures have to be corrected for the thermal pressure increase, ΔP_{th}. We measured ΔP_{th} at 20.4 GPa and 2000 K using both ruby and strontium borate chips in the vicinity of the heated micro-furnace and obtained $+0.8 \pm 0.2$ GPa, the same as in our previous study [2].

Because accurate pressure measurements are key to the determination of the steep mineral phase boundaries, we performed new measurements of the thermal pressures for our present diamond cell configuration. ΔP_{th} depends on the temperature, the geometry of the sample assembly, and the size of the hot spot. The latter two were kept nearly the same for all present experiments. Because fluorescence becomes very weak above about 700 K, fluorescence peaks can only be measured from the outer portion of the hot spot. Ruby is unsuitable for accurate measurements of ΔP_{th} due to the large temperature shift of the fluorescence spectrum. We demonstrate, however, in separate experiments using helium and argon as pressure media, that the fluorescence peak of strontium borate has negligible shift with temperature up to at least 700 K (see also [35]) and that its shift during heating must therefore be only due to the thermal pressure increase, ΔP_{th}. In these experiments a mixture of fine-grained (1–3 μm) ruby and strontium borate chips was pressed into a thin (<10 μm) rhenium or iridium foil (Fig. 2A) and fluorescence spectra from adjacent ruby and strontium borate chips were measured throughout the sample chamber during and after laser heating. Fig. 2B,C shows the shifts of the fluorescence peaks, $\Delta\lambda = (\lambda - \lambda_0)$ (nm), of the ruby R_1 line (circles) and the $SrB_4O_7{:}Sm^{2+}$ $^7D_0 - {}^5F_0$ line (diamonds) vs. distance (μm) from the center of the hot spot ($\lambda_0 = 694.2$ nm for ruby and $\lambda_0 = 685.4$ nm for strontium borate). Solid

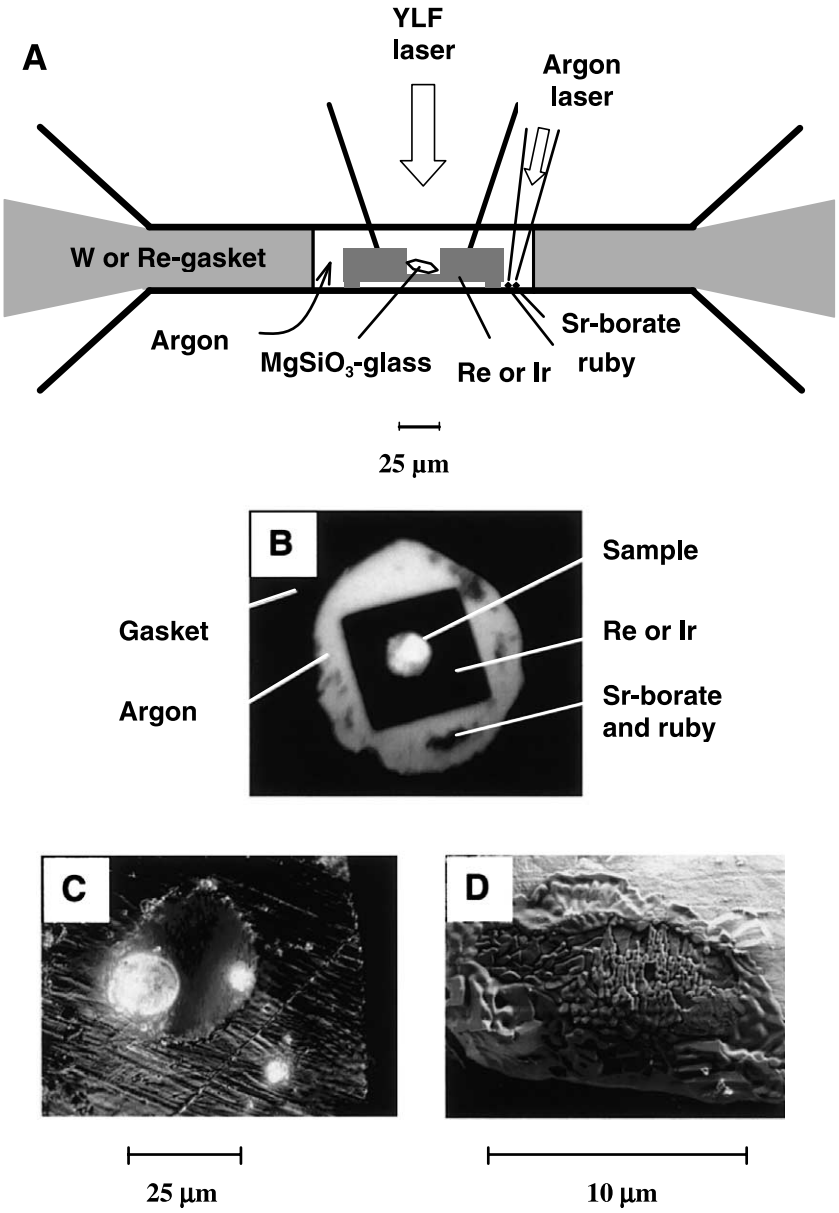

Fig. 1. Schematics of diamond-anvil cell used in this study. (A) Cross-section of a sample chamber. Chips of $MgSiO_3$-glass with dimensions of 10–15 μm were placed into micro-furnaces (rhenium or iridium) 100–120 μm in diameter and 30 μm thickness. Culets were 400 μm, and gasket (tungsten or rhenium) holes 160–180 μm in diameter. Argon was used as pressure medium. Pressures and thermal pressure increases were measured from adjacent grains of ruby and strontium borate excited with an argon laser. (B) Sample during laser heating at 22.4 GPa and about 2600 K (run 3). (C) Recovered sample of B after melting showing sphere of perovskite (see Raman spectrum in Fig. 3). (D) SEM image of $MgSiO_3$-garnet (run 12-2) showing features of melting and recrystallization.

Table 1
Results of phase transitions in $MgSiO_3$

Run	p[a] (GPa)	T (K)	Heating duration (min)	Run products[b]
2-1	19.8 ± 0.2	2160 ± 60	15	Ak
2-3	20.8 ± 0.2	2140 ± 100	20	Ak
2-4	21.3 ± 0.3	2150 ± 50	13	Ak
2-6	22.3 ± 0.2	2130 ± 60	23	Ak
2-7	23.5 ± 0.2	2150 ± 40	13	Ak+Pv
2-9	24.5 ± 0.1	2130 ± 60	20	Ak+Pv
2-10	22.5 ± 0.2	2190 ± 50	30	Ak+Pv
2-11	21.7 ± 0.2	2140 ± 80	25	Ak+Pv
2-12	21.2 ± 0.1	2160 ± 100	25	Ak+Pv
2-13	20.1 ± 0.2	2140 ± 80	60	Ak+Pv
2-14	19.6 ± 0.2	2170 ± 120	50	Ak+W+St+Pv
2-15	19.0 ± 0.2	2200 ± 90	30	Ak+W+St
2-16	20.9 ± 0.2	2400 ± 20	15	Ak+W+St+Pv
2-17	21.3 ± 0.2	2400 ± 50	15	Ak+W+St+Pv
2-18	22.2 ± 0.2	2340 ± 60	20	Pv
2-20	21.2 ± 0.2	2380 ± 60	25	Pv
2-21	20.5 ± 0.2	2360 ± 40	25	Pv
2-22	19.9 ± 0.2	2370 ± 50	20	W+St
2-23	19.7 ± 0.2	2460 ± 30	20	Pv
2-24	20.5 ± 0.1	2490 ± 60	10	Pv
2-25	20.0 ± 0.1	2480 ± 60	10	Pv
3	21.3 ± 0.3	just below melting	15	Pv
9	20.0 ± 0.1	just below melting	10	Pv
12-1	19.6 ± 0.3	2300 ± 70	15	W+St
12-2	19.7 ± 0.3	just below melting	5	Maj
13-1	19.7 ± 0.2	2240 ± 100	25	Ak+W+St
13-2	23.2 ± 0.1	2000 ± 60	15	Ak+Pv
13-3	21.3 ± 0.1	1990 ± 60	20	Ak+Pv
13-4	20.0 ± 0.2	1960 ± 70	40	Ak+Pv
13-5	18.9 ± 0.1	2000 ± 50	20	Ak
13-6	18.5 ± 0.1	2410 ± 50	8	Maj
13-7	18.7 ± 0.1	2470 ± 50	7	Maj
13-8	19.6 ± 0.1	2510 ± 40 (signs of melting)	7	Maj
14-1	17.8 ± 0.1	2300 ± 20	5	Maj
14-2	19.8 ± 0.1	2440 ± 30	8	Maj
14-3	19.6 ± 0.2	2500 ± 90 (signs of melting)	5	Maj
15-1	20.6 ± 0.1	2110 ± 90	17	Ak
15-2	20.9 ± 0.1	2280 ± 30	10	Pv
17-1	21.2 ± 0.2	1900 ± 60	20	Ak
17-3	21.8 ± 0.1	1930 ± 30	20	Ak
17-4	22.5 ± 0.1	2050 ± 50	20	Ak
17-5	22.5 ± 0.1	2160 ± 80	15	Pv
18-1	22.8 ± 0.3	2060 ± 100	15	Pv
18-3	19.5 ± 0.2	1990 ± 70	25	Pv
18-4	18.3 ± 0.1	2000 ± 30	20	Pv+Ak
19-1	22.1 ± 0.1	1930 ± 40	15	Ak
19-2	22.7 ± 0.1	2020 ± 30	12	Ak+Pv
19-3	22.7 ± 0.1	2110 ± 20	18	Ak+Pv
23-1	21.8 ± 0.1	2010 ± 50	35	Ak
23-2	21.8 ± 0.1	2090 ± 100	20	Ak
24-1	23.4 ± 0.1	2100 ± 50	25	Pv
24-2	20.4 ± 0.2	2110 ± 60	90	Pv+Ak

Table 1 (*Contents*).

Run	p[a] (GPa)	T (K)	Heating duration (min)	Run products[b]
25-1	22.1 ± 0.3	1840 ± 40	30	Ak
25-2	22.1 ± 0.3	1970 ± 60	20	Ak
25-3	22.1 ± 0.2	2040 ± 60	25	Ak
25-4	22.2 ± 0.2	2110 ± 50	30	Ak+Pv
26-1	22.1 ± 0.1	1940 ± 40	20	Ak+Pv
26-2	19.2 ± 0.2	2120 ± 80	15	Ak
26-3	20.5 ± 0.1	2220 ± 20	10	Ak
26-4	20.5 ± 0.1	2270 ± 40	12	Ak
26-5	20.6 ± 0.2	2340 ± 30	10	Ak+W+St+Pv

[a] Pressures measured after heating without thermal pressure correction.
[b] For abbreviations see Fig. 3.

symbols show $\Delta\lambda$ during laser heating, and open symbols after quenching. In the helium run the pressure was 11.4 GPa, measured from both ruby and strontium borate. At this pressure helium is liquid at room temperature [36]. As expected, no pressure gradient throughout the pressure chamber was observed at room temperature. During heating, the temperature in the center of a hot spot was directly measured as 1700 K and dropped below about 1100 K at a distance of about 50 μm from the center. Outside this area temperatures could not be measured with our spectrometer but due to the high thermal conductivity in the metal foil the strontium borate and ruby chips are subject to substantial temperature gradients. The fluorescence peaks of strontium borate all show the same shift during heating throughout the pressure chamber, whereas the ruby peaks show strong temperature dependence. Therefore we assume that the peak shifts of strontium borate are only due to the thermal pressure increase, and ΔP_{th} was calculated to be 0.9 ± 0.06 GPa.

The ruby fluorescence line may also be used for estimating ΔP_{th}, but this method is less accurate because the temperature of the ruby chips has to be estimated from the measured broadening of the ruby R_1 line and its reported temperature dependence [37,38]. The calculated temperature shift of the ruby peak then has to be subtracted from the total peak shift in order to obtain ΔP_{th} [2,35,37]. The resulting value for ΔP_{th} of 1 GPa has a large uncertainty of about ±0.25 GPa, but ΔP_{th} agrees with the value obtained from strontium borate.

In Fig. 2C we verify previous measurements [33,39] of the relaxation of pressure gradients in an argon pressure medium resulting from laser heating. Both ruby and strontium borate show a uniform pressure distribution after heating the sample. During heating, at a peak sample temperature of 2300 K, ΔP_{th} calculated from the fluorescence shift of strontium borate was 1.8 ± 0.1 GPa. This value is higher than in the present phase transition runs due to a substantially larger ratio of the heated sample volume to argon volume in this experiment.

The phase diagram of $MgSiO_3$ was measured in the temperature range 1800–2600 K but for the present cell configuration ΔP_{th} was only measured at 2000 K. The temperature dependence of ΔP_{th} was calculated from $\alpha K_T \Delta T$, where α is the thermal expansion coefficient, K_T is the bulk modulus, and ΔT is the temperature increase. Assuming that αK_T is approximately constant over the present temperature range [40], ΔP_{th} is proportional to the temperature. This means that ΔP_{th} at 2600 K should increase to 1.1 GPa compared to 0.8 GPa at 2000 K. From the observed relaxation of pressure gradients in the argon pressure medium and the measure thermal pressures we estimate the uncertainty in our reported pressures as ±0.2 GPa.

The method of temperature measurement by fitting the Planck radiation function to the measured emission spectra is described in detail elsewhere [33]. Temperature uncertainties listed in Table 1 are mainly from temperature fluctuations during heating. Systematic errors of about 100 K

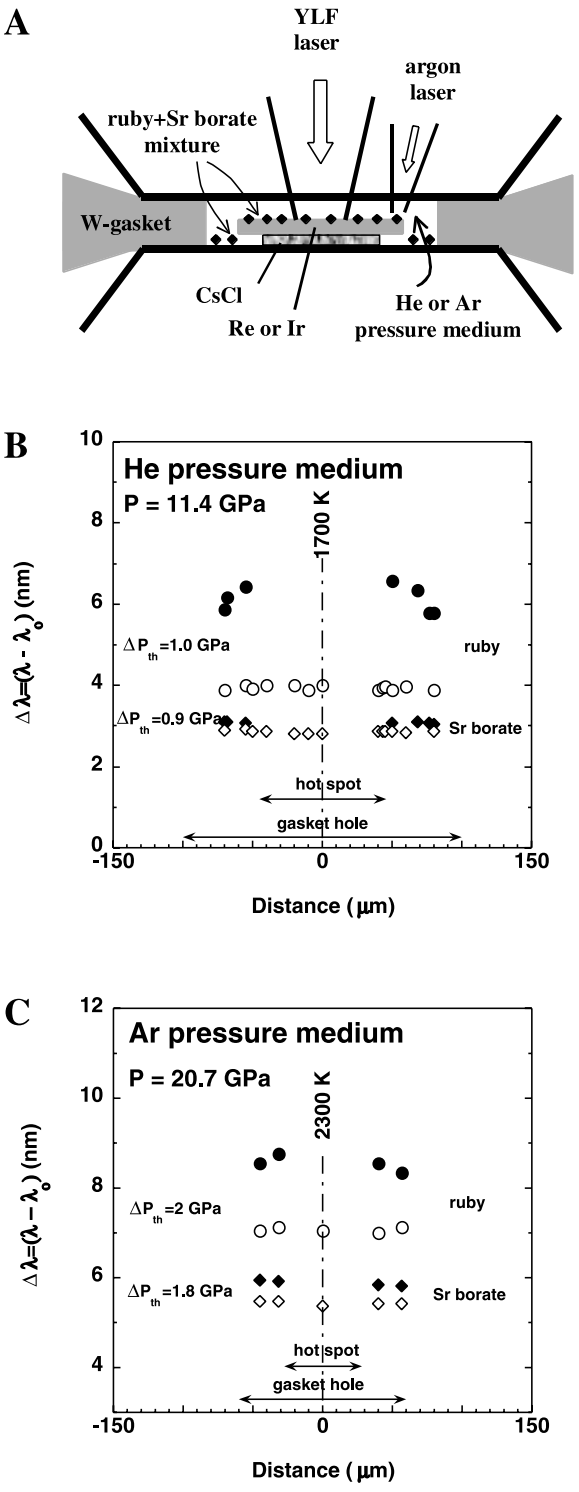

may be added if the emissivity–wavelength relation is significantly different from that of a graybody [33] (temperatures and emissivities are obtained from the Planck function assuming wavelength-independent emissivities).

Sixty heating cycles with subsequent Raman measurements of the temperature-quenched samples were performed in 14 runs and are shown in chronological order in Table 1. All five phases, akimotoite, majorite, Mg–Si-perovskite, wadsleyite, and stishovite, were identified unambiguously (Fig. 3). The data shown in Table 1 are plotted in Fig. 4 after applying thermal pressure corrections between +0.7 and +1.1 GPa, depending on temperature.

Equilibrium phase boundaries are commonly determined by midpoints of forward and reverse transitions between two phases. Reverse transition have often been proven to be technically difficult and have been measured only recently for the $MgSiO_3$ system [19,20]. In this study we report 11 forward and six reversal runs. Additionally we report 14 direct transformations from glass starting material. In the present study forward transitions from akimotoite to perovskite are runs 2-7, 15-2, 17-5, 19-2, 25-4, and 26-5. Reverse transitions from perovskite to akimotoite are 13-5, 18-4, 24-2, and 26-2. Very obviously at the lower temperatures of this study the hysteresis for these transitions is very large, and a precise determination of the equilibrium phase boundary is not possible. This large hysteresis is likely due to the absence of shear forces in a hydrostatic (molten argon) pressure medium, an effect previously studied in detail for iron [41] and also observed for olivine [23,42,43]. It is clear, however, from runs 26-4 to 26-5 and a reversal transition of pe-

←

Fig. 2. Fluorescence shifts of two pressure calibrants, ruby and strontium borate, measured during and after laser heating in diamond cell. (A) Schematic cross-section of a sample chamber. (B) Fluorescence shifts of ruby and strontium borate measured in a helium pressure medium at 11.4 GPa during laser heating (peak temperature 1700 K) and after quenching. (C) Fluorescence shifts of ruby and strontium borate measured in an argon pressure medium at 20.7 GPa during laser heating (peak temperature 2300 K) and after quenching.

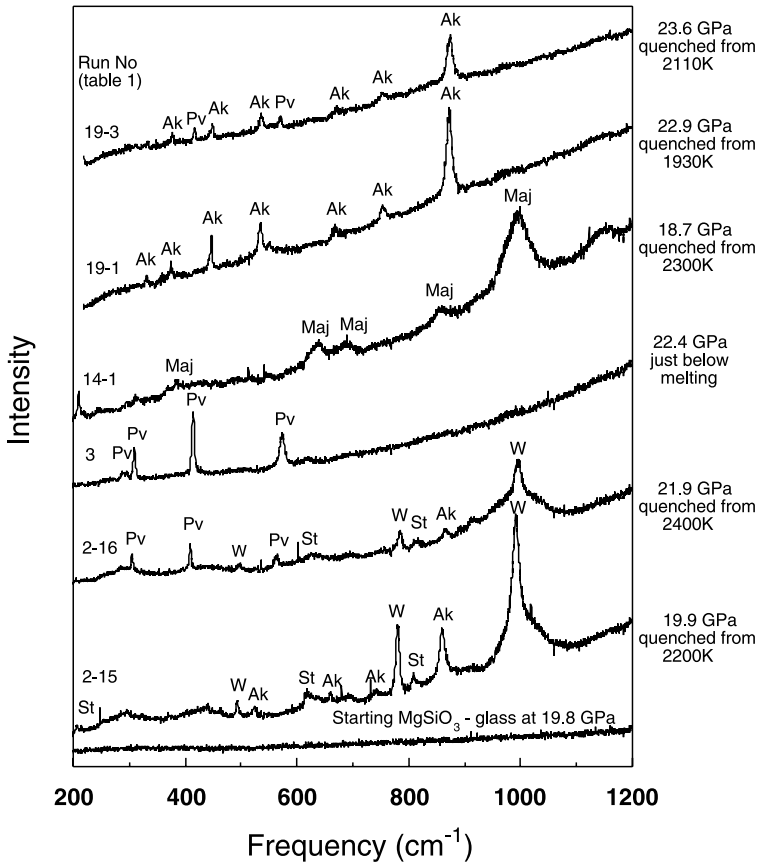

Fig. 3. Raman spectra of the phases subject to the phase diagram shown in Fig. 4 after laser heating at high pressures. All peak positions agree with high pressure Raman data shown in the literature. Ak = akimotoite [1,49,59], Pv = perovskite [1,49], Maj = $MgSiO_3$-garnet [1,49,60], W = Mg_2SiO_4 β-spinel (wadsleyite) [61], St = stishovite [62].

rovskite to wadsleyite+stishovite (runs 2-21 to 2-22) that at these higher temperatures kinetic effects are significantly smaller and the triple point akimotoite–wadsleyite+stishovite–perovskite must be at around 21 GPa and 2300 K, indicated by the circle in Fig. 4 in which all four phases have been observed. This triple point and the forward and reverse transitions listed above give upper and lower pressure bounds for the akimotoite–perovskite phase boundary indicated by dashed lines in Fig. 4.

Additional data points by directly transforming the glass starting material to either ilmenite or perovskite are obtained from runs 2-1, 15-1, 17-1, 18-1, 19-1, 23-1, 25-1, and 26-1. The validity of these data points, however, may be questionable because glass starting materials do not necessarily produce the most thermodynamically stable phase according to Ostwald's step rule, which states that phase transitions proceed through a series of intermediate phases, each thermodynamically more stable than the preceding (Ostwald, 1897, in [44]). This process is controlled by the kinetics of nucleation and/or crystal growth [44,45]. Nevertheless, glass starting materials have been used in recent studies avoiding kinetic problems to determine phase boundaries [21,29,46,47]. The main reason for using glass starting material instead of enstatite in the present study is overlap of the most intensive Raman modes of akimotoite and perovskite with some of those of enstatite [1,48,49].

It has been shown that both glassy and crystalline starting materials produced the thermodynamically stable phase [47,50]. If the data points

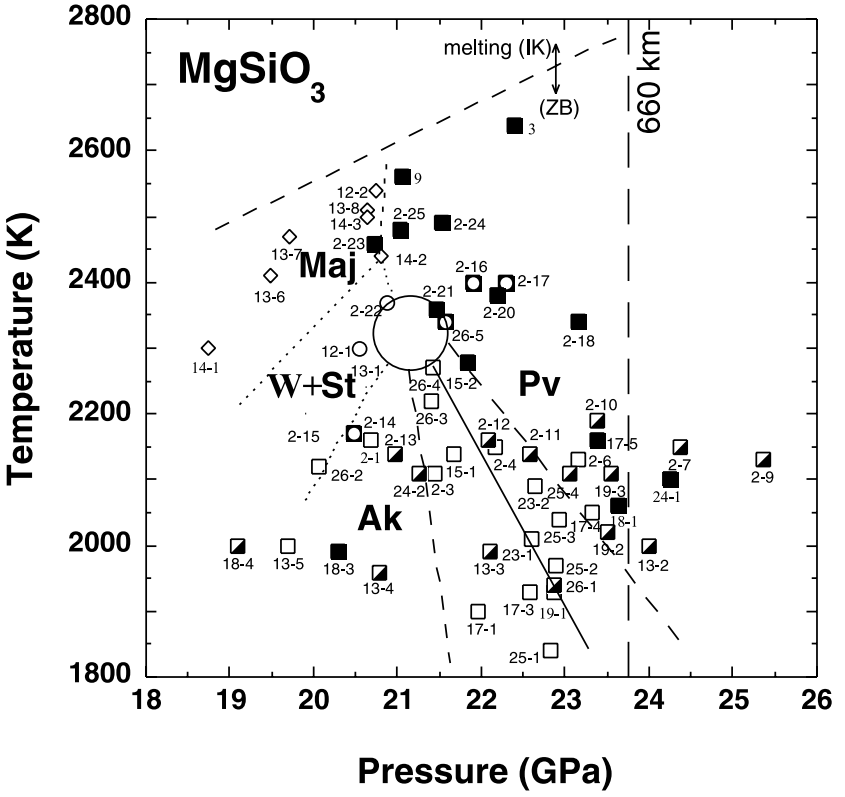

Fig. 4. Phase diagram of $MgSiO_3$. The pressures listed in Table 1 were corrected for thermal pressure by between +0.7 and +1.1 GPa (see text). Open squares are akimotoite, solid squares are perovskite, open circles are wadsleyite plus stishovite, open diamonds are majorite ($MgSiO_3$-garnet), and mixed symbols represent mixed run products. The run numbers are listed in Table 1. The circle indicates the triple point akimotoite–wadsleyite+stishovite–perovskite. Dashed lines show upper and lower bounds for the akimotoite–perovskite phase boundary from reversal experiments and the solid line is the best fit of this boundary to data using glass starting material. Dotted lines indicate the approximate location of wadsleyite+stishovite stability field. Dashed line is the majorite–perovskite phase boundary. Melting curve is shown as an average from Ito and Katsura [16] and Zerr and Boehler [63].

using glass starting materials are included in the present work the slope of the phase boundary between akimotoite and perovskite would be -0.004 ± 0.002 GPa/K as indicated by the solid line in Fig. 4. At high temperature this boundary is anchored by the akimotoite–wadsleyite+stishovite–perovskite triple point and at lower temperatures by run 26-1.

The stability field of wadsleyite+stishovite is not well constrained because this was not the primary objective of this work. Its approximate location is indicated by dotted lines and the akimotoite–wadsleyite+stishovite–perovskite triple point.

For the majorite–perovskite boundary above 2400 K there are no direct forward or reverse runs to determine the phase boundary. However, the fact that only pure phases were observed over a narrow pressure range led us to conclude that phase kinetics play a minor role at these high temperatures and that equilibrium was in fact achieved in the reported heating durations. The resulting phase boundary is nearly vertical at 21 GPa.

3. Discussion

In Fig. 5 our results are compared with those of previous multi-anvil experiments and those calcu-

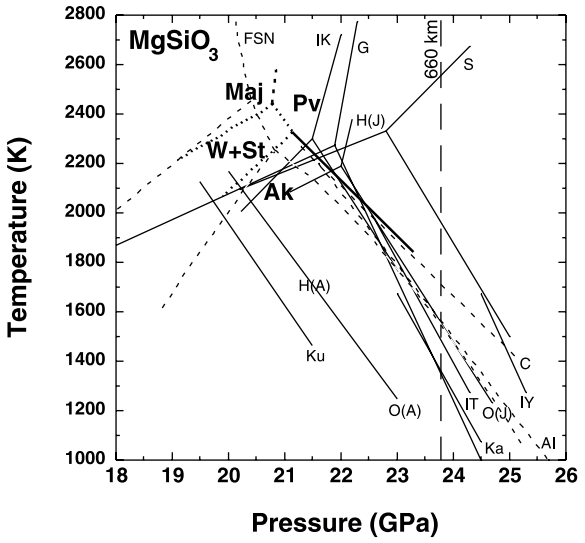

Fig. 5. Comparison of measured and calculated $MgSiO_3$ phase boundaries. Thick lines = this work. Thin solid lines – from experiments: S = Sawamoto [13], IK = Ito and Katsura [16], G = Gasparik [14], Ku = Kuroda et al. [19], Ka = Kato et al.[17], IT = Ito and Takahashi [5], IY = Ito and Yamada [12], O = Ono et al. [20] (below 1673 K), H = Hirose et al. [21] (above 1673 K), (A) = Anderson et al.'s [24] equation of state of gold was used for pressure calibration, (J) = Jamieson at al.'s [25] equation was used. Thin dashed lines – from calculations: C = Chopelas [49], FSN = Fei et al. [57], AI = Akaogi and Ito [52].

lated from thermodynamic and spectroscopic data. Including all data points of our work, the slope of the akimotoite–perovskite phase boundary of this study, -0.004 ± 0.002 GPa/K, is in agreement within the reported uncertainties with those from multi-anvil quench experiments [5,12–16,21] and from in situ X-ray measurements [17,19–21] ranging from -0.002 to -0.003 GPa/K. With several exceptions [13–16,21] these experiments were performed at lower temperatures (1000–1800 K) [5,12,17,19,20]. Our slope is consistent with those calculated from calorimetric measurements (-0.005 ± 0.002 GPa/K [51], -0.003 ± 0.002 GPa/K [52]) and from spectroscopic data (-0.005 GPa/K [49]).

For comparison, the Clapeyron slope of the ringwoodite to perovskite+periclase transition in the Mg_2SiO_4 system, as observed in most multi-anvil and laser-heated diamond-anvil studies [2,3,5,11,12,14,15,23], is slightly smaller. It lies in the range from -0.001 to -0.003 GPa/K. This difference in slope between these two systems implies that the boundaries of these two Mg–Si-perovskite reactions would intersect at some (lower) temperature. This would imply that below that temperature, for compositions between pure $MgSiO_3$ and Mg_2SiO_4, ringwoodite would break down to akimotoite plus periclase and not to perovskite plus periclase. This possibility was predicted for the $MgO–SiO_2$ system from computer simulations [53], and akimotoite plus periclase was obtained in experiments with $MgSiO_3$ composition at 23 GPa and 1500°C [54]. It is, however, equally likely that the two phase boundaries converge at low temperature as was shown for the CMAS system ($CaO–MgO–Al_2O_3–SiO_2$) [15].

In summary, the present and most previous studies on the slopes of Mg–Si-perovskite forming transitions in both Mg_2SiO_4 and $MgSiO_3$ systems range from -0.001 to -0.004 GPa/K. Thus, these transitions are unlikely to induce layering in mantle convection because for layering to occur in a convecting mantle with an endothermic phase boundary, Clapeyron slopes between -0.004 and -0.008 GPa/K are required [7,8].

The akimotoite–perovskite phase boundary, at the pressure equivalent to 660 km depth (23.8 GPa), yields a temperature of about 1800 K, nearly the same as that of the ringwoodite to perovskite+periclase transition in the Mg_2SiO_4 system (1900 ± 100 K) [1–3], suggesting that this transition would also contribute to the observed jump in seismic velocities. The role of ilmenite in the post-spinel transitions relevant to 660 km depth, however, is controversial [5,12–15,17,20,21,46,47,55,56], which will not be further discussed here.

The nearly vertical boundary of the majorite–perovskite transition suggests that majorite is not stable at lower mantle conditions. Our measurements are in good agreement with general predictions based on entropies and densities of these phases [9] and thermodynamic calculations [57]. However, some of the previous experiments [13–16,21] show the presence of $MgSiO_3$-garnet up to higher pressures and positive Clapeyron slopes between garnet and perovskite, but the transition "was not precisely determined" [21], but was cal-

culated using the calorimetric measurements [58]. With regard to the stability of garnets it is interesting to note that the laser-heated diamond cell study on the stability field of $Mg_3Al_2Si_3O_{12}$-pyrope [55] has shown that pure pyrope is not stable at lower mantle conditions, but instead the stability field of Al-bearing akimotoite is expanded to higher temperatures comparing to end-member $MgSiO_3$-akimotoite. However, other studies using quenching methods in multi-anvil presses showed that pyrope is stable up to about 26 GPa and then dissociates into aluminous perovskite solid solution plus corundum solid solution [28,46,47]. Moreover, for pyrolite composition it was found [30–32] that majoritic garnet coexists with a lower mantle mineral assemblage (aluminous $MgSiO_3$-rich perovskite, $CaSiO_3$-rich perovskite, and magnesiowüstite) at the uppermost part of the lower mantle (at 24–25 GPa and 1600°C). It was observed that phase kinetics in the transition pyrope–akimotoite–perovskite are very slow under hydrostatic conditions below about 2200 K [55] and therefore this system requires additional reversal experiments using a variety of experimental methods.

Acknowledgements

We thank J. Huth for his assistance in taking SEM images, D. Yuen and V. Hillgren for helpful discussions. Thanks to H. O'Neill for a constructive review. Financial support for L.C. from the Deutsche Forschungsgemeinschaft is acknowledged. *[BW]*

References

[1] R. Boehler, A. Chopelas, Phase transitions in a 500 kbar-3000 K gas apparatus, in: Y. Syono, M.H. Manghnani (Eds.), High-Pressure Research: Application to Earth and Planetary Sciences, Terra, Tokyo, 1992, pp. 55–60.

[2] L. Chudinovskikh, R. Boehler, High-pressure polymorphs of olivine and the 660-km seismic discontinuity, Nature 411 (2001) 574–577.

[3] S.-H. Shim, T.S. Duffy, G. Shen, The post-spinel transformation in Mg_2SiO_4 and its relation to the 660-km seismic discontinuity, Nature 411 (2001) 571–574.

[4] L. Liu, The post-spinel phase of forsterite, Nature 262 (1976) 770–772.

[5] E. Ito, E. Takahashi, Postspinel transformations in the system Mg_2SiO_4-Fe_2SiO_4 and some geophysical implications, J. Geophys. Res. 94 (1989) 10637–10646.

[6] R. Boehler, A. Chopelas, A new approach to laser heating in high pressure mineral physics, Geophys. Res. Lett. 18 (1991) 1147–1150.

[7] U.R. Christensen, D.A. Yuen, The interaction of a subducting lithospheric slab with a chemical or phase boundary, J. Geophys. Res. 89 (1984) 4389–4402.

[8] U.R. Christensen, D.A. Yuen, Layered convection induced by phase transitions, J. Geophys. Res. 90 (1985) 10291–10300.

[9] A. Navrotsky, Lower mantle phase transitions may generally have negative pressure-temperature slopes, Geophys. Res. Lett. 7 (1980) 709–711.

[10] W. Zhao, D.A. Yuen, S. Honda, Multiple phase transitions and the style of mantle convection, Phys. Earth Planet. Inter. 72 (1992) 185–210.

[11] A. Chopelas, R. Boehler, T. Ko, Thermodynamics and behavior of γ-Mg_2SiO_4 at high pressure: Implications for Mg_2SiO_4 phase equilibrium, Phys. Chem. Miner. 21 (1994) 351–359.

[12] E. Ito, H. Yamada, Stability relations of silicate spinels, ilmenites, and perovskites, in: S. Akimoto, M.H. Manghnani (Eds.), High Pressure Research in Geophysics, Center of Academic Publications, Tokyo, 1982, pp. 225–266.

[13] H. Sawamoto, Phase diagram of $MgSiO_3$ at pressures up to 24 GPa and temperatures up to 2200°C: phase stability and properies of tetragonal garnet, in: M.H. Manghnani, Y. Syono (Eds.), High-Pressure Research in Mineral Physics, Terra, Tokyo, 1987, pp. 209–219.

[14] T. Gasparik, Phase relations in the transition zone, J. Geophys. Res. 95 (1990) 15751–15769.

[15] T. Gasparik, Melting experiments on the enstatite-diopside join at 70–224 kbar, including the melting of diopside, Contrib. Mineral. Petrol. 124 (1996) 139–153.

[16] E. Ito, T. Katsura, Melting of ferromagnesian silicates under the lower mantle conditions, in: Y. Syono, M.H. Manghnani (Eds.), High-Pressure Research: Application to Earth and Planetary Sciences, Terra, Tokyo, 1992, pp. 315–322.

[17] T. Kato, E. Ohtani, H. Morishima, D. Yamazaki et al., In situ X ray observation of high-pressure phase transitions of $MgSiO_3$ and thermal expansion of $MgSiO_3$ perovskite at 25 GPa by double-stage multianvil system, J. Geophys. Res. 100 (1995) 20475–20481.

[18] T. Irifune, N. Nishiyama, K. Kuroda, T. Inoue et al., The postspinel phase boundary in Mg_2SiO_4 determined by in situ X-ray diffraction, Science 279 (1998) 1698–1700.

[19] K. Kuroda, T. Irifune, T. Inoue, N. Nishiyama et al., Determination of the phase boundary between ilmenite and perovskite in $MgSiO_3$ by in situ X-ray diffraction and quench experiments, Phys. Chem. Miner. 27 (2000) 523–532.

[20] S. Ono, T. Katsura, E. Ito, M. Kanzaki et al., In situ observation of ilmenite-perovskite phase transition in $MgSiO_3$ using synchrotron radiation, Geophys. Res. Lett. 28 (2001) 835–838.
[21] K. Hirose, T. Komabayashi, M. Murakami, K. Funakoshi, In situ measurements of the majorite-akimotoite-perovskite phase transition boundaries in $MgSiO_3$, Geophys. Res. Lett. 22 (2001) 4351–4354.
[22] K. Hirose, Phase transitions in pyrolitic mantle around 670-km depth: Implications for upwelling of plumes from the lower mantle, J. Geophys. Res. 107 (B4) (2002) doi:2010.1029/2001JB000597.
[23] T. Katsura, H. Yamada, T. Shinmei, A. Kubo et al., Post-spinel transition in Mg_2SiO_4 determined by high P-T in situ X-ray diffractometry, Phys. Earth Planet. Inter. 136 (2003) 11–24.
[24] O.L. Anderson, D.G. Isaak, S. Yamamoto, Anharmonicity and the equation of state of gold, J. Appl. Phys. 65 (1989) 1534–1543.
[25] J.C. Jamieson, J.N. Fritz, M.N. Manghnani, Pressure measurement at high temperature in x-ray diffraction studies: gold as a primary standard, in: S. Akimoto, M.H. Manghnani (Eds.), High Pressure Research in Geophysics, Center of Academic Publications, Tokyo, 1982, pp. 27–48.
[26] D.L. Decker, High pressure equation of state for NaCl, KCl, and CsCl, J. Appl. Phys. 42 (1971) 3239–3244.
[27] T. Irifune, Application of synchrotron radiation and Kawai-type apparatus to various studies in high-pressure mineral physics, Mineral. Mag. 66 (2002) 769–790.
[28] T. Irifune, T. Koizumi, J. Ando, An experimental study of the garnet-perovskite transition in the system $MgSiO_3$-$Mg_3Al_2Si_3O_{12}$, Phys. Earth Planet. Inter. 96 (1996) 147–157.
[29] K. Hirose, Y. Fei, S. Ono, T. Yagi et al., In situ measurements of the phase transition boundary in $Mg_3Al_2Si_3O_{12}$: implications for the nature of the seismic discontinuities in the Earth's mantle, Earth Planet. Sci. Lett. 184 (2001) 567–573.
[30] T. Irifune, Absence of an aluminous phase in the upper part of the Earth's lower mantle, Nature 370 (1994) 131–133.
[31] N. Nishiyama, T. Yagi, Phase relation and mineral chemistry in pyrolite to 2200°C under the lower mantle pressures and implications for dynamics of mantle plumes, J. Geophys. Res. 108 (2003) 2255–2267.
[32] B.J. Wood, Phase transformations and partitioning relations in peridotite under lower mantle conditions, Earth Planet. Sci. Lett. 174 (2000) 341–354.
[33] R. Boehler, High-pressure experiments and the phase diagram of lower mantle and core materials, Rev. Geophys. 38 (2000) 221–245.
[34] S.-H. Shim, T.S. Duffy, T. Kenichi, Equation of state of gold and its application to the phase boundaries near 660 km depth in Earth's mantle, Earth Planet. Sci. Lett. 203 (2002) 729–739.
[35] F. Datchi, R. Le Toullec, P. Loubeyre, Improved calibration of the SrB_4O_7:Sm^{2+} optical pressure gauge: Advantages at very high pressures and high temperatures, J. Appl. Phys. 81 (1997) 3333–3339.
[36] F. Datchi, P. Loubeyre, R. Le Toullec, Extended and accurate determination of the melting curves of argon, helium, ice (H_2O), and hydrogen (H_2), Phys. Rev. B 61 (2000) 6535–6546.
[37] O. Shimomura, S. Yamaoka, H. Nakazawa, O. Fukunaga, Application of a diamond-anvil cell to high-temperature and high-pressure experiments, in: S. Akimoto, M.H. Manghnani (Eds.), High Pressure Research in Geophysics, Center for Academic Publishing of Japan, Tokyo, 1982, pp. 49–60.
[38] D.D. Ragan, R. Gustavsen, D. Shiferl, Calibration of ruby R1 and R2 fluorecsence shift as a function of temperature from 0 to 600 K, J. Appl. Phys. 72 (1992) 5539–5544.
[39] G. Serghiou, A. Zerr, L. Chudinovskikh, R. Boehler, The coesite-stishovite transition in a laser-heated diamond cell, Geophys. Res. Lett. 22 (1995) 441–444.
[40] O.L. Anderson, A universal thermal equation of state, J. Geodyn. 1 (1984) 185–214.
[41] R. Boehler, N. von Bargen, A. Chopelas, Melting, thermal expansion, and phase transitions of iron at high hydrostatic pressures, J. Geophys. Res. 95 (1990) 21731–21737.
[42] P.C. Burnley, H.W. Green II, Stress dependence of the mechanism of the olivine-spinel transformation, Nature 338 (1989) 753–756.
[43] A.J. Brearley, D.C. Rubie, E. Ito, Mechanisms of the transformations between the α, β and γ polymorphs of Mg_2SiO_4 at 15 GPa, Phys. Chem. Miner. 18 (1992) 343–358.
[44] J.W. Morse, W.H. Casey, Ostwald processes and mineral paragenesis in sediments, Am. J. Sci. 288 (1988) 537–560.
[45] J. Renner, A. Zerbian, B. Stöckhert, Microstructures of synthetic polycrystalline coesite aggregates. The effect of pressure, temperature, and time, Lithos 41 (1997) 169–184.
[46] A. Kubo, M. Akaogi, Post-garnet transitions in the system $Mg_4Si_4O_{12}$-$Mg_3Al_2Si_3O_{12}$ up to 28 GPa: phase relations of garnet, ilmenite and perovskite, Phys. Earth Planet. Inter. 121 (2000) 85–102.
[47] M. Akaogi, A. Tanaka, E. Ito, Garnet-ilmenite-perovskite transitions in the system $Mg_4Si_4O_{12}$-$Mg_3Al_2Si_3O_{12}$ at high pressures and high temperatures: phase equilibria, calorimetry and implications for mantle structure, Phys. Earth Planet. Inter. 132 (2002) 303–324.
[48] A. Chopelas, R. Boehler, Raman spectroscopy of high pressure $MgSiO_3$ phases synthesized in a CO_2 laser heated diamond anvil cell: perovskite and clinopyroxene, in: Y. Syono, M.H. Manghnani (Eds.), High-Pressure Research: Application to Earth and Planetary Sciences, Terra, Tokyo, 1992, pp. 101–108.
[49] A. Chopelas, Estimates of mantle relevant Clapeyron slopes in the $MgSiO_3$ system from high-pressure spectroscopic data, Am. Mineral. 84 (1999) 233–244.

[50] M. Akaogi, S. Akimoto, Pyroxene-garnet solid-solution equilibria in the systems $Mg_4Si_4O_{12}$–$Mg_3Al_2Si_3O_{12}$ and $Fe_4Si_4O_{12}$–$Fe_3Al_2Si_3O_{12}$ at high pressures and temperatures, Phys. Earth Planet. Inter. 15 (1977) 90–106.

[51] E. Ito, M. Akaogi, L. Topor, A. Navrotsky, Negative pressure-temperature slopes for reactions forming $MgSiO_3$ perovskite from calorimetry, Science 249 (1990) 1275–1278.

[52] M. Akaogi, E. Ito, Refinement of enthalpy measurements of $MgSiO_3$ perovskite and negative pressure-temperature slopes for perovskite-forming reactions, Geophys. Res. Lett. 20 (1993) 1839–1842.

[53] O.L. Kuskov, O.B. Fabrichnaya, R.F. Galimzyanov, L.M. Truskinovsky, Computer simulation of the phase diagram for the MgO-SiO_2 system at P-T parameters of the mantle transition zone, Phys. Chem. Miner. 16 (1989) 442–454.

[54] T. Irifune, A.E. Ringwood, Phase transformations in a harzburgite composition to 26 GPa: implications for dynamical behaviour of the subducted slab, Earth Planet. Sci. Lett. 86 (1987) 365–367.

[55] G. Serghiou, A. Zerr, A. Chopelas, R. Boehler, The transition of pyrope to perovskite, Phys. Chem. Miner. 25 (1998) 193–196.

[56] P. Vacher, A. Mocquet, C. Sotin, Computation of seismic profiles from mineral physics: the importance of the non-olivine components for explaining the 660 km depth discontinuity, Phys. Earth Planet. Inter. 106 (1998) 275–298.

[57] Y. Fei, S.K. Saxena, A. Navrotsky, Internally consistent thermodynamic data and equilibrium phase relations for compounds in the system MgO-SiO_2 at high pressure and high temperature, J. Geophys. Res. 95 (1990) 6915–6928.

[58] M. Akaogi, E. Ito, Calorimetric study on majorite-perovskite transition in the system $Mg_4Si_4O_{12}$-$Mg_3Al_2Si_3O_{12}$: transition boundaries with positive pressure-temperature slopes, Phys. Earth Planet. Inter. 114 (1999) 129–140.

[59] B. Reynard, D.C. Rubie, High-pressure, high-temperature Raman spectroscopic study of ilmenite-type $MgSiO_3$, Am. Mineral. 81 (1996) 1092–1096.

[60] P. McMillan, M. Akaogi, E. Ohtani, Q. Williams et al., Cation disorder of garnets along the $Mg_3Al_2Si_3O_{12}$ - $Mg_4Si_4O_{12}$ join: an IR, RAMAN and NMR study, Phys. Chem. Miner. 16 (1989) 428–435.

[61] A. Chopelas, Thermal properties of β-Mg_2SiO_4 at mantle pressures derived from vibrational spectroscopy: Implications for the mantle at 400 km depth, J. Geophys. Res. 96 (1991) 11817–11829.

[62] R.J. Hemley, Pressure dependence of Raman spectra of SiO_2 polymorphs: α-quartz, coesite, and stishovite, in: M.H. Manghnani, Y. Syono (Eds.), High-Pressure Research in Mineral Physics, Terra, Tokyo, 1987, pp. 347–359.

[63] A. Zerr, R. Boehler, Melting of (Mg,Fe)SiO_3-perovskite to 625 kilobars: Indication of a high melting temperature in the lower mantle, Science 262 (1993) 553–555.